

Optical control of an atomic inner-shell x-ray laser

Gábor Darvasi,¹ Christoph H. Keitel,¹ and Christian Buth^{1,2,*}

¹Max-Planck-Institut für Kernphysik, Saupfercheckweg 1, 69117 Heidelberg, Germany

²Argonne National Laboratory, Argonne, Illinois 60439, USA

(Dated: 08 March 2013)

X-ray free-electron lasers have had an enormous impact on x-ray science by achieving femtosecond pulses with unprecedented intensities. However, present-day facilities have a number of shortcomings, namely, their radiation has a chaotic pulse profile and short coherence times. We put forward a scheme for a neon-based atomic inner-shell x-ray laser (XRL) which produces temporally and spatially coherent, sub-femtosecond pulses that are controlled by and synchronized to an optical laser with femtosecond precision. We envision that such an XRL will allow for numerous applications such as nuclear quantum optics and the study of ultrafast quantum dynamics of atoms, molecules, and condensed matter.

PACS numbers: 42.55.Vc, 32.80.Aa, 32.80.Rm, 41.60.Cr

An x-ray laser (XRL) is an old goal of laser physics [1–3]. Extending the superior coherence, intensity and controlled pulse properties of lasers to the x-ray regime has the potential to revolutionize x-ray science by bringing unprecedented intensities, temporal and spatial control of beam properties, and ultrashort pulses to the x-ray scientist. A solution of this problem renders XRLs suitable for numerous applications from ionic and nuclear quantum optics [4, 5] to high-energy and astrophysics [6, 7] and it offers perspectives for the measurement and control of quantum dynamics of matter on an ultrafast time scale [8, 9]. X-ray free-electron-lasers (FELs) [10, 11] such as the Linac Coherent Light Source (LCLS) [12, 13] have reached several of the goals laid out for XRLs, namely, ultraintense, tunable, femtosecond x-ray pulses. However, present-day x-ray FELs operate by the principle of self-amplified spontaneous emission (SASE) [12–16] and thus suffer from a number of shortcomings compared with optical lasers. Specifically, they lack controllability of the pulse properties, spectral narrowness, and photon energy stability [12, 13]. Furthermore, there is a jitter between SASE radiation and an optical laser which can only be determined with a several tens of femtoseconds precision [17].

Lasing schemes from the optical regime cannot be transferred simply to the x-ray regime due to the unfavorable scaling of the cross section for stimulated emission [1], the lack of high-reflectivity mirrors for x rays [2], and the short duration of population inversion caused by inner-shell decay [18]. Lasing in the XUV and soft x-ray regime has been accomplished with plasma-based XRLs via collisional or recombinational pumping [2, 3]. However, these techniques have not yet reached beyond the water window starting at 276.2 eV.

A different scheme for x-ray lasing in the kiloelectronvolt regime was proposed by Duguay and Rentzepis in 1967 [19] based on atomic inner-shell transitions in core-ionized atoms. Our modified Duguay-and-Rentzepis scheme where the atoms are core excited is illustrated

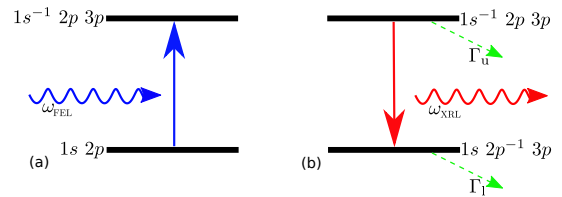


FIG. 1. (Color online) Schematic of x-ray lasing in neon with pumping by an x-ray FEL. (a) Neon atoms are excited by x rays from an FEL. (b) X-ray lasing occurs. Further, Γ_U and Γ_L are the decay widths of the upper and lower lasing states, respectively.

in Fig. 1. An intense x-ray beam is focused into a gas cell with atoms. At a given photon energy above the inner-shell edge, tightly bound inner-shell electrons are much more likely to interact with x rays than electrons in other shells [18]. First, atoms are core-excited producing a state of population inversion in the propagation direction of the x-ray pulse [19]. Second, photons are emitted through spontaneous radiative decay of some of the core-excited atoms. Third, these photons propagate along the medium and induce stimulated x-ray emission from other core-excited ions further downstream in straight conceptual analogy to optical lasers [1]. Due to longitudinal pumping, x-ray lasing only occurs in the propagation direction of the pump pulse [20–22]. Until recently it was not possible to realize such an XRL due to the high x-ray intensity [23, 24] necessary to excite the lasing medium faster than inner-shell holes decay.

The advent of XUV and x-ray FELs has reinvigorated interest in this scheme producing a number of theoretical studies [20–22, 25] and the experimental realization for neon in 2011 at LCLS [26]. Although this simple, uncontrolled XRL scheme produces pulses with a single, fully coherent intensity spike, it still suffers from a number of shortcomings: the pulse properties strongly depend on the temporal shape of the pump pulse and multicolor lasing may occur [20–22] due to x-ray lasing on transitions

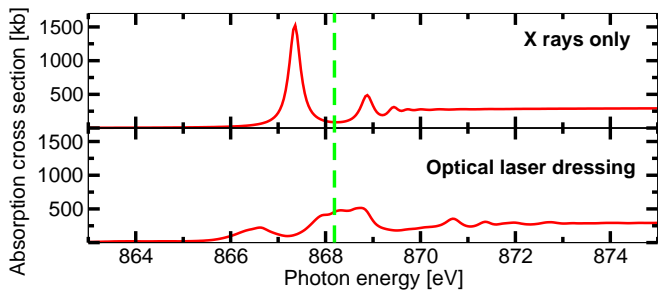


FIG. 2. (Color online) X-ray absorption cross section of neon near the K edge for the field-free case (top) and for optical laser dressing at 10^{13} W/cm² (bottom) with an 800 nm laser. The x rays and the optical light are linearly polarized and have parallel polarization vectors. The dashed, green line indicates the central x-ray FEL photon energy at $\omega_P = 868.2$ eV. Adapted from Ref. 27.

in highly charged ions. Multiple, simultaneous, uncontrolled pulses may lead to complications in experiments harnessing the XRL light.

We put forward an XRL scheme for neon that is controlled by optical light [Fig. 1]. The x-ray FEL photon energy $\omega_P = 868.2$ eV is tuned below the K edge slightly above the $1s \rightarrow 1s^{-1}3p$ resonance, as indicated by the dashed, green line in the x-ray absorption cross section in Fig. 2. For the FEL x rays, the core excitation is off-resonant and thus inefficient [Fig. 2a], if the bandwidth of the FEL x rays is limited sufficiently, e.g., by self-seeding techniques [28]. X-ray lasing occurs on the superposition of $1s^{-1}2p3p \rightarrow 1s2p^{-1}3p$ and $1s^{-1}2p4p \rightarrow 1s2p^{-1}4p$ transitions leading to a two-peak feature around 849 eV for highly monochromatized x rays [29]. We assume a FWHM bandwidth of the FEL x rays of $\Delta\omega_P = 0.4$ eV which causes a broadened x-ray emission feature. A copropagating optical laser modulates the x-ray absorption cross section $\sigma^{1s}(I_L, \omega)$ [27, 30–35] as shown in Fig. 2 which thus becomes dependent on the optical laser intensity I_L . At ω_P , the $\sigma^{1s}(I_L, \omega)$ is increased more than sixfold from 86 to 510 kilobarns when I_L is increased from zero to 10^{13} W/cm² at 800 nm wavelength which allows a high degree of control over the absorption of the FEL x rays and thus the population inversion. Also, the optical laser rapidly ionizes Rydberg electrons such as the $3p$ electron via multiphoton processes leading to a large induced width for Rydberg electrons of approximately 0.54 eV [27] and a mixture of core-excited and core-ionized atoms is found in the gas cell. For core-ionized neon atoms, the x-ray emission spectrum [36] peaks at $\omega_X = 848.66$ eV which is within the linewidth of the emission from core-excited states [29]. Therefore, we need not distinguish between core-excited [29] and core-ionized [36] neon atoms. The lifetime of the upper state is only minutely influenced by the presence of a Rydberg electron [37] and is $\tau_A = 2.4$ fs imply-

ing an XRL linewidth from core-ionized atoms of $\Delta\omega = 0.27$ eV [38]. Furthermore, optical laser ionization, Auger decay, and the very short coherence time of SASE x rays cause strong decoherence making semiclassical laser theory [1] applicable to understand the effect of optical laser dressing on x-ray lasing.

The small-signal gain (SSG) [1, 20–22] represents the amplification of spontaneously emitted x rays on the XRL transition in the exponential gain regime:

$$g(t) = \sigma_{se} N_U(t) - \sigma_{abs} N_L(t), \quad (1)$$

where $N_U(t)$ is the upper-level occupancy, $N_L(t)$ is the lower-level occupancy, and σ_{se} and σ_{abs} are the stimulated emission and absorption cross sections, respectively, with

$$\sigma_{se} = A_{U \rightarrow L} \frac{2\pi c^2}{\omega^2 \Delta\omega}, \quad \sigma_{abs} = \sigma_{se} \frac{g_U}{g_L}, \quad (2)$$

where $A_{U \rightarrow L} = 5.9 \times 10^{12}$ s⁻¹ is the Einstein coefficient for spontaneous emission on the XRL transition, and $g_U = 6$ and $g_L = 1$ are the probabilistic weights of the upper and lower laser levels, respectively, in our case. The cross sections in Eq. (2) have been evaluated at the peak of the line, assuming a Lorentzian line shape [20–22].

We generate SASE x-ray FEL pulses with the partial-coherence method [39–41] with a Gaussian spectrum centered at ω_P with FWHM of $\Delta\omega_P = 0.4$ eV. The x-ray FEL beam is assumed Gaussian with a waist of $w_0 = 10$ μ m [12, 13]. We place the neon atoms in a gas cell around the beam waist with a length of $L = 5$ mm. In Fig. 3a, we show optical laser pulses [42] at three different positions with respect to a single SASE x-ray FEL pulse; in Fig. 3b we display the SSG for pumping with this SASE pulse with and without optical laser dressing for each of the three positions. A pronounced modulation of the SSG occurs only for the dashed, red optical laser pulse. The SSG is modified substantially only if the optical laser pulse overlaps with the rising flank of the x-ray FEL pulse. Otherwise, the K -shell absorption cross section is modified either too early—before the x rays from the FEL interact with the atoms—or too late, after a substantial fraction of the atoms has already been destroyed, i.e., excited or ionized.

As the shape of the x-ray pulse from a SASE FEL varies on a shot-to-shot basis [15, 16], we present SSG results averaged over 500 single-shot calculations in Fig. 3b for the three positions of the optical dressing laser. The average SASE pulse over 500 shots is shown in Fig. 3a. The importance of the relative timing between the x-ray FEL pulse and the optical laser pulse is also reflected in the averaged calculations. The average SSG increases from $0.16 a_0^2$ to $0.4 a_0^2$ for the optical laser pulse drawn dashed, red in Fig. 3a while no substantial increase of the SSG is observed for the dashed, blue and dashed, green positions of the optical laser pulse. It is apparent

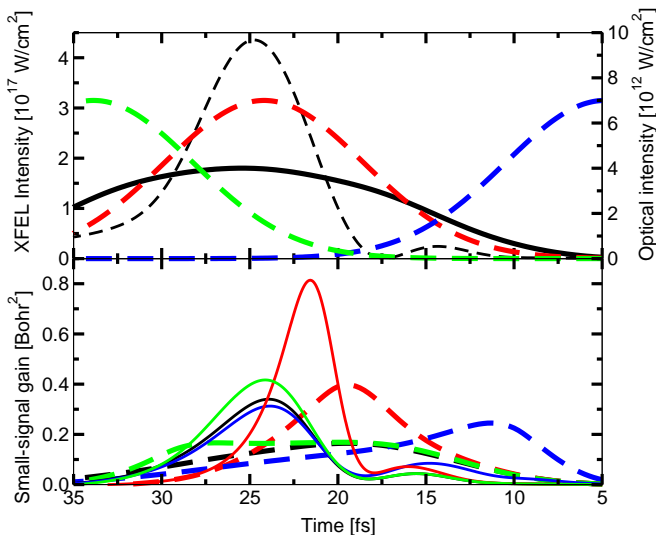


FIG. 3. (Color) (a) The dashed, black line is the amplitude of a single SASE pulse. The dashed, red, blue, and green lines are the optical dressing laser at three different positions with respect to the SASE pulse. The solid, black line is the average over 500 SASE pulses. We assume 3×10^{13} x rays in, on average, 50 fs FWHM long pulses, focused to a $10 \mu\text{m}$ spot at a bandwidth of 0.4 eV. (b) The solid, black line shows the single-shot SSG in the field-free case when the XRL is pumped with the single, dashed, black SASE pulse from (a) which has a FWHM duration of 7.3 fs; the solid, red, blue, and green lines show the single-shot SSG for laser dressing with the optical laser pulse of matching color from (a). The average of the SSG over 500 SASE pulses for the field-free case is given by the dashed, black line and for optical laser dressing by the dashed, red, blue, and green lines.

in Fig. 3b that some temporal control over the XRL is possible. The peak of the averaged SSG is shifted in the direction of the optical dressing laser for each of the three cases. The modulation of the SSG results from the increase of the K -shell absorption cross section by optical laser dressing as seen in Fig. 2, and the rate at which the upper level population and the population inversion are built up. However, the optical laser does not affect processes that destroy the population inversion, namely, the decay rates of the upper level and the rate of valence ionization which also reduce the occupancy of the upper level. Therefore, optical laser dressing allows for the build-up of a larger population inversion than in the field-free case.

Based on the analysis of the SSG it seems feasible to control the XRL with a copropagating optical laser. In order to find out its impact we need to determine the output of the XRL based on single-shot calculations of the XRL intensity $I_X(z, t)$. To determine the occupancy of the upper lasing level $N_U(z, t)$ at position z as a function of time t , we need to consider all processes that build up or remove population, namely, photoexcitation and valence ionization by the x-ray FEL pulse, sponta-

neous and stimulated emission, and Auger decay. Different frequency components of the x-ray FEL pulse excite the atoms at varying rates due to the strong variation of $\sigma^{1s}(I_L, \omega)$ around the x-ray FEL central frequency ω_P , see Fig. 2. Therefore, to obtain the photoexcitation rate, one needs to calculate the convolution of the absorption cross section $\sigma^{1s}(I_L, \omega)$ and the spectral intensity $S_P(z, \omega)$ [43] of the x-ray FEL pulse. The rate equation for $N_U(z, t)$ is given by

$$\begin{aligned} \frac{dN_U(z, t)}{dt} = & \frac{I_P(z, t)}{\omega_P} N_S(z, t) \frac{\int_0^\infty \sigma^{1s}(I_L, \omega) \frac{S_P(z, \omega)}{\omega} d\omega}{\int_0^\infty \frac{S_P(z, \omega)}{\omega} d\omega} \\ & - \frac{\sigma_{se}}{\omega_X} I_X(z, t) N_U(z, t) + \frac{\sigma_{abs}}{\omega_X} I_X(z, t) N_L(z, t) \\ & - [\Gamma_A + A_{U \rightarrow L} + \sigma_U^{\text{tot}} \frac{I_P(z, t)}{\omega_P}] N_U(z, t), \quad (3) \end{aligned}$$

where $N_S(z, t)$ is the population of the neon ground state, $\Gamma_A = 3.8 \times 10^{14} \text{s}^{-1}$ is the Auger decay rate of the upper lasing level, and $\sigma_U^{\text{tot}} = 32.8 \text{ kilobarn}$ [44, 45] is the total absorption cross section of the upper lasing level for x rays from the FEL. The first line on the right-hand side of Eq. (3) represents the rate at which the upper level is populated via photoexcitation. We specify the x-ray FEL photon flux by $\frac{I_P(z, t)}{\omega_P}$, because $\frac{\Delta\omega_P}{\omega_P} = 5 \times 10^{-4} \ll 1$. The first term in the second line of the right-hand side accounts for transitions due to stimulated emission induced by the XRL light from the upper to the lower lasing state and the second term describes the absorption of XRL light by atoms in the lower lasing state promoting them to the upper state. The bottom line of Eq. (3) describes the processes that remove population from the upper level, namely spontaneous emission, Auger decay, and valence ionization by the x rays of the FEL. The occupancy $N_S(z, t)$ of the ground state and the occupancy $N_L(z, t)$ of the lower lasing state are determined analogously by rate equations [46].

Depending on the occupancy of the upper and lower states of the XRL, light is either attenuated or amplified in the medium. The XRL intensity is coupled to the occupancies by

$$\begin{aligned} \frac{dI_X(z, t)}{dz} = & I_X(z, t) c n_{\#} [\sigma_{se} N_U(z, t) - \sigma_{abs} N_L(z, t)] \quad (4) \\ & + \omega_X \frac{\Omega(z)}{4\pi} A_{U \rightarrow L} N_U(z, t) c n_{\#} - c \frac{dI_X(z, t)}{dz}, \end{aligned}$$

where c is the speed of light in vacuum and $n_{\#}$ is the atomic number density. Only photons emitted into $\Omega(z) = 2\pi [1 - (L-z)/\sqrt{w_0^2 + (L-z)^2}]$ contribute to x-ray lasing [20–22]. The first line on the right-hand side of Eq. (4) describes stimulated emission and absorption of light from the XRL pulse. The first term in the last line of Eq. (4) is the rate of spontaneous emission which initiates x-ray lasing in the forward direction whereas the second term represents the propagation of the XRL x rays.

We apply Eqs. (3) and (4) to our XRL and calculate $I_X(z, t)$ in dependence of the propagation distance

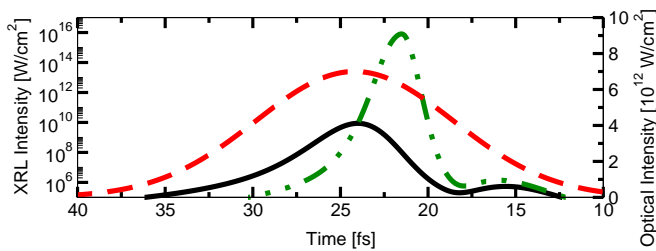


FIG. 4. (Color online) The temporal profile of the XRL pulses after saturation pumped with the dashed, black FEL pulse from Fig. 3a. The solid, black line corresponds to the FEL-x-rays-only case and the dot-dashed, green line displays the optically laser-dressed case by the dashed, red optical laser pulse from Fig. 3a, which is shown by the dashed, red line.

in the gas cell for $n_{\#} = 10^{19} \text{ cm}^{-3}$. The temporal profile of the XRL pulse for laser dressing with the dashed, red optical laser pulse is shown in Fig. 4. The small peak at the front of the XRL pulse is ascribed to emission processes from a small population inversion caused by the small peak in the x-ray FEL pulse found at approximately 15 fs in Fig. 3a. The comparison of the solid and dot-dashed lines reveals that optical laser dressing leads to an increase by about six orders of magnitude in the XRL's peak intensity. Since the XRL's intensity is correlated with the SSG, which in turn depends on the K -shell absorption cross section, it is possible to control the XRL's intensity via the peak intensity of the optical dressing laser, which determines the magnitude of the change in the absorption cross section.

The FWHM duration of the XRL pulse from the FEL-x rays-only case in Fig. 4 is compressed from 2.0 fs down to 0.7 fs when the dashed, red optical laser pulse is used. The reason for the compression of the pulse is that optical laser dressing facilitates a faster build-up of population inversion resulting in its reduced temporal length. All XRL photons are emitted within a shorter time period; the photons from the first and last emission process are closer to each other. Furthermore, it is seen in Fig. 4 that the output of the optically laser-dressed XRL is synchronized to the optical laser pulse with an accuracy of less than 5 fs.

In conclusion, the XRL scheme presented here allows one to produce controlled, fully coherent, single peak x-ray pulses with intensities above 10^{16} W/cm^2 that are synchronized to an optical laser pulse with femtosecond accuracy. It thus opens up perspectives for two-color pump-probe experiments. The optically controlled XRL offers a novel way to measure the time jitter between SASE radiation and an optical laser at present-day facilities. Namely, by placing a filter behind the gas cell that absorbs an intensity of up to 10^{11} W/cm^2 , the output of the FEL x-ray-only XRL can be entirely absorbed. Then, XRL output is only generated when the optical laser pulse overlaps with the front of the x-ray FEL pulse.

This allows to determine the overlap between x rays and the optical laser with femtosecond precision. Multicolor x-ray lasing on several transitions, as predicted for a core-ionization-pumped XRL [20–22] may not occur because the x-ray FEL photon energy is too low to core-ionize neon cations. Above all, the optically controlled XRL facilitates to imprint the transverse intensity profile of the optical laser pulse onto the XRL pulse.

We would like to thank Stefano M. Cavaletto for fruitful discussions. C.B. was supported by the Chemical Sciences, Geosciences, and Biosciences Division of the Office of Basic Energy Sciences, Office of Science, U.S. Department of Energy, under Contract No. DE-AC02-06CH11357.

* Corresponding author; christian.buth@web.de

- [1] P. W. Milonni and J. H. Eberly, *Laser physics*, 2nd ed. (John Wiley & Sons, Hoboken, New Jersey, 2010).
- [2] S. Suckewer and P. Jaeglé, *Laser Phys. Lett.* **6**, 411 (2009).
- [3] J. J. Rocca, *Rev. Sci. Instrum.* **70**, 3799 (1999).
- [4] B. W. Adams, C. Buth, S. M. Cavaletto, J. Evers, Z. Harman, C. H. Keitel, A. Pálffy, A. Picón, R. Röhlberger, Y. Rostovtsev, and T. Kenji, *J. Mod. Opt.* **60**, 2 (2013).
- [5] R. Röhlberger, H.-C. Wille, K. Schlage, and B. Sahoo, *Nature* **482**, 199 (2012).
- [6] A. Di Piazza, C. Müller, K. Z. Hatsagortsyan, and C. H. Keitel, *Rev. Mod. Phys.* **84**, 1177 (2012).
- [7] S. Bernitt, G. V. Brown, J. K. Rudolph, R. Steinbrügge, A. Graf, M. Leutenegger, S. W. Epp, S. Eberle, K. Kubiček, V. Mäkel, M. C. Simon, E. Träbert, E. W. Magee, C. Beilmann, N. Hell, S. Schippers, A. Müller, S. M. Kahn, A. Surzhykov, Z. Harman, C. H. Keitel, J. Clementson, F. S. Porter, W. Schlotter, J. J. Turner, J. Ullrich, P. Beiersdorfer, and J. R. Crespo López-Urrutia, *Nature* **492**, 225 (2012).
- [8] F. Krausz and M. Ivanov, *Rev. Mod. Phys.* **81**, 163 (2009).
- [9] S. M. Cavaletto, Z. Harman, C. Buth, and C. H. Keitel, submitted (2013), arXiv:1302.3141.
- [10] J. M. J. Madey, *J. Appl. Phys.* **42**, 1906 (1971).
- [11] E. L. Saldin, E. A. Schneidmiller, and M. V. Yurkov, *The physics of free electron lasers* (Springer, Berlin, Heidelberg, New York, 2000).
- [12] J. Arthur, P. Anfinrud, P. Audebert, K. Bane, I. Ben-Zvi, V. Bharadwaj, R. Bionta, P. Bolton, M. Borland, P. H. Bucksbaum, R. C. Cauble, J. Clendenin, M. Cornacchia, G. Decker, P. Den Hartog, S. Dierker, D. Dowell, D. Dungan, P. Emma, I. Evans, G. Faigel, R. Falcone, W. M. Fawley, M. Ferrario, A. S. Fisher, R. R. Freeman, J. Frisch, J. Galayda, J.-C. Gauthier, S. Gierman, E. Gluskin, W. Graves, J. Hajdu, J. Hastings, K. Hodgson, Z. Huang, R. Humphry, P. Ilinski, D. Imre, C. Jacobsen, C.-C. Kao, K. R. Kase, K.-J. Kim, R. Kirby, J. Kirz, L. Klaisner, P. Krejcik, K. Kulanter, O. L. Landen, R. W. Lee, C. Lewis, C. Limborg, E. I. Lindau, A. Lumpkin, G. Materlik, S. Mao, J. Miao, S. Mochrie, E. Moog, S. Milton, G. Mulholland, K. Nel-

- son, W. R. Nelson, R. Neutze, A. Ng, D. Nguyen, H.-D. Nuhn, D. T. Palmer, J. M. Paterson, C. Pellegrini, S. Reiche, M. Renner, D. Riley, C. V. Robinson, S. H. Rokni, S. J. Rose, J. Rosenzweig, R. Ruland, G. Ruocco, D. Saenz, S. Sasaki, D. Sayre, J. Schmerge, D. Schneider, C. Schroeder, L. Serafini, F. Sette, S. Sinha, D. van der Spoel, B. Stephenson, G. Stupakov, M. Sutton, A. Szöke, R. Tatchyn, A. Toor, E. Trakhtenberg, I. Vasserman, N. Vinokurov, X. J. Wang, D. Waltz, J. S. Wark, E. Weckert, Wilson-Squire Group, H. Winick, M. Woodley, A. Wootton, M. Wulff, M. Xie, R. Yotam, L. Young, and A. Zewail, *Linac coherent light source (LCLS): Conceptual design report*, SLAC-R-593, UC-414 (2002) www-ssrl.slac.stanford.edu/lcls/cdr.
- [13] P. Emma, R. Akre, J. Arthur, R. Bionta, C. Bostedt, J. Bozek, A. Brachmann, P. Bucksbaum, R. Coffee, F.-J. Decker, Y. Ding, D. Dowell, S. Edstrom, J. Fisher, A. Frisch, S. Gilevich, J. Hastings, G. Hays, P. Hering, Z. Huang, R. Iverson, H. Loos, M. Messerschmidt, A. Miahnahri, S. Moeller, H.-D. Nuhn, G. Pile, D. Ratner, J. Rzepiela, D. Schultz, T. Smith, P. Stefan, H. Tompkins, J. Turner, J. Welch, W. White, J. Wu, G. Yocky, and J. Galayda, *Nature Photon.* **4**, 641 (2010).
- [14] I. A. Vartanyants, A. Singer, A. P. Mancuso, O. M. Yefanov, A. Sakdinawat, Y. Liu, E. Bang, G. J. Williams, G. Cadenazzi, B. Abbey, H. Sinn, D. Attwood, K. A. Nugent, E. Weckert, T. Wang, D. Zhu, B. Wu, C. Graves, A. Scherz, J. J. Turner, W. F. Schlotter, M. Messerschmidt, J. Lüning, Y. Acremann, P. Heimann, D. C. Mancini, V. Joshi, J. Krzywinski, R. Soufli, M. Fernandez-Perea, S. Hau-Riege, A. G. Peele, Y. Feng, O. Krupin, S. Moeller, and W. Wurth, *Phys. Rev. Lett.* **107**, 144801 (2011).
- [15] R. Bonifacio, C. Pellegrini, and L. M. Narducci, *Opt. Commun.* **50**, 373 (1984).
- [16] A. M. Kondratenko and E. L. Saldin, *Dokl. Akad. Nauk SSSR* **249**, 843 (1979), [*Sov. Phys. Dokl.* **24**, 986-988 (1979)].
- [17] S. Schorb, T. Gorkhover, J. P. Cryan, J. M. Glowina, M. R. Bionta, R. N. Coffee, B. Erk, R. Boll, C. Schmidt, D. Rolles, A. Rudenko, A. Rouzee, M. Swiggers, S. Carron, J.-C. Castagna, J. D. Bozek, M. Messerschmidt, W. F. Schlotter, and C. Bostedt, *Appl. Phys. Lett.* **100**, 121107 (2012).
- [18] J. Als-Nielsen and D. McMorrow, *Elements of modern x-ray physics* (John Wiley & Sons, New York, 2001).
- [19] M. A. Duguay and P. M. Rentzepis, *Appl. Phys. Lett.* **10**, 350 (1967).
- [20] N. Rohringer and R. London, *Phys. Rev. A* **80**, 013809 (2009).
- [21] N. Rohringer and R. London, *Phys. Rev. A* **82**, 049902(E) (2010).
- [22] N. Rohringer, *J. Phys.: Conf. Ser.* **194**, 012012 (2009).
- [23] H. C. Kapteyn, *Photoionization-pumped short-wavelength lasers*, PhD thesis, University of California, Berkeley, California (1989), jila.colorado.edu/~kapteyn/Research/Thesis%20formatted.pdf
- [24] H. C. Kapteyn, *Appl. Opt.* **31**, 4931 (1992).
- [25] K. Lan, E. Fill, and J. Meyer-ter-Vehn, *Laser Part. Beams* **22**, 261 (2004).
- [26] N. Rohringer, D. Ryan, R. A. London, M. Purvis, F. Albert, J. Dunn, J. D. Bozek, C. Bostedt, A. Graf, R. Hill, S. P. Hau-Riege, and J. J. Rocca, *Nature* **481**, 488 (2012).
- [27] C. Buth, R. Santra, and L. Young, *Phys. Rev. Lett.* **98**, 253001 (2007), arXiv:0705.3615.
- [28] J. Amann, W. Berg, V. Blank, F.-J. Decker, Y. Ding, P. Emma, Y. Feng, J. Frisch, D. Fritz, J. Hastings, Z. Huang, J. Krzywinski, R. Lindberg, H. Loos, A. Lutman, H.-D. Nuhn, D. Ratner, J. Rzepiela, D. Shu, Y. Shvyd'ko, S. Spampinati, S. Stoupin, S. Terentyev, E. Trakhtenberg, D. Walz, J. Welch, J. Wu, A. Zholents, and D. Zhu, *Nature Photon.* **6**, 693 (2012).
- [29] M. Oura, *Plasma Sci. Technol.* **12**, 353 (2010).
- [30] R. Santra, C. Buth, E. R. Peterson, R. W. Dunford, E. P. Kanter, B. Krässig, S. H. Southworth, and L. Young, *J. Phys.: Conf. Ser.* **88**, 012052 (2007), arXiv:0712.2556.
- [31] H. R. Varma, L. Pan, D. R. Beck, and R. Santra, *Phys. Rev. A* **78**, 065401 (2008).
- [32] R. Santra, R. W. Dunford, E. P. Kanter, B. Krässig, S. H. Southworth, and L. Young, in *Advances in Atomic, Molecular, and Optical Physics*, Vol. 56, edited by E. Arimondo, P. R. Berman, and C. C. Lin (Academic Press, Amsterdam, 2008) pp. 219–259.
- [33] C. Buth, R. Santra, and L. Young, *Rev. Mex. Fís. S* **56**, 59 (2010), arXiv:0805.2619.
- [34] L. Young, C. Buth, R. W. Dunford, P. J. Ho, E. P. Kanter, B. Krässig, E. R. Peterson, N. Rohringer, R. Santra, and S. H. Southworth, *Rev. Mex. Fís. S* **56**, 11 (2010), arXiv:0809.3537.
- [35] T. E. Glover, M. P. Hertlein, S. H. Southworth, T. K. Allison, J. van Tilborg, E. P. Kanter, B. Krässig, H. R. Varma, B. Rude, R. Santra, A. Belkacem, and L. Young, *Nature Phys.* **6**, 69 (2010).
- [36] H. Ågren, J. Nordgren, L. Selander, C. Nordling, and K. Siegbahn, *J. Electron Spectrosc. Relat. Phenom.* **14**, 27 (1978).
- [37] A. De Fanis, N. Saito, H. Yoshida, Y. Senba, Y. Tamenori, H. Ohashi, H. Tanaka, and K. Ueda, *Phys. Rev. Lett.* **89**, 243001 (2002).
- [38] V. Schmidt, *Electron spectrometry of atoms using synchrotron radiation* (Cambridge University Press, Cambridge, 1997).
- [39] T. Pfeifer, Y. Jiang, S. Düsterer, R. Moshhammer, and J. Ullrich, *Opt. Lett.* **35**, 3441 (2010).
- [40] Y. H. Jiang, T. Pfeifer, A. Rudenko, O. Herrwerth, L. Foucar, M. Kurka, K. U. Kühnel, M. Lezius, M. F. Kling, X. Liu, K. Ueda, S. Düsterer, R. Treusch, C. D. Schröter, R. Moshhammer, and J. Ullrich, *Phys. Rev. A* **82**, 041403(R) (2010).
- [41] S. M. Cavaletto, C. Buth, Z. Harman, E. P. Kanter, S. H. Southworth, L. Young, and C. H. Keitel, *Phys. Rev. A* **86**, 033402 (2012), arXiv:1205.4918.
- [42] The beam waist of the optical laser is chosen sufficiently large to ensure a confocal parameter that is larger than L .
- [43] J.-C. Diels and W. Rudolph, *Ultrashort laser pulse phenomena*, 2nd ed., Optics and Photonics Series (Academic Press, Amsterdam, 2006).
- [44] Los Alamos National Laboratory, Atomic Physics Codes, aphysics2.lanl.gov/tempweb/lanl.
- [45] R. D. Cowan, *The theory of atomic structure and spectra*, Los Alamos Series in Basic and Applied Sciences (University of California Press, Berkeley, 1981).
- [46] G. Darvasi, *Optical control of x-ray lasing*, Diplomarbeit, Ruprecht-Karls-Universität Heidelberg, Max-Planck-Institut für Kernphysik, Saupfercheckweg 1, 69117 Heidelberg, Germany (2011), urn:nbn:de:bsz:16-opus-132045, www.ub.uni-heidelberg.de/archiv/13204.